Neuroinformatics

Editors

Giorgio A. Ascoli

Erik De Schutter

David N. Kennedy

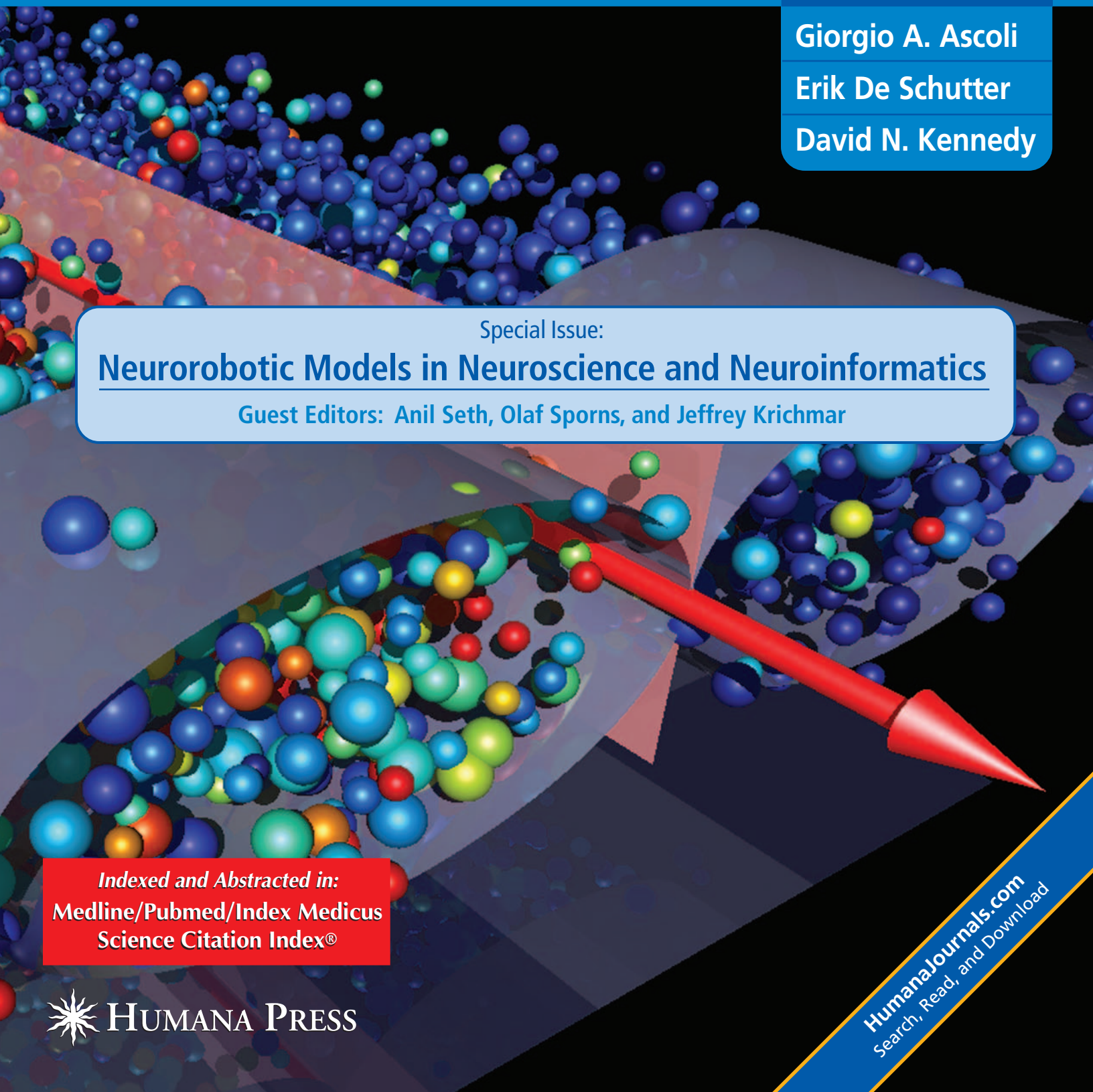

Special Issue:

Neurorobotic Models in Neuroscience and Neuroinformatics

Guest Editors: Anil Seth, Olaf Sporns, and Jeffrey Krichmar

Indexed and Abstracted in:
Medline/Pubmed/Index Medicus
Science Citation Index®

HUMANA PRESS

Neuroinformatics

1539-2791/05/171–196/$30.00
DOI: 10.1385/NI:3:3:171

Original Article

Simulation and Robotics Studies of Salamander Locomotion

Applying Neurobiological Principles to the Control of Locomotion in Robots

Auke Jan Ijspeert,[*,1] *Alessandro Crespi,*[1] *and Jean-Marie Cabelguen*[2]

[1]Swiss Federal Institute of Technology, Lausanne (EPFL), Station 14, CH-1015, Lausanne, Switzerland; and [2]Inserm E 358, Institut Magendie, 1 rue C. St-Saëns, F-33077 Bordeaux, France

Abstract

This article presents a project that aims at understanding the neural circuitry controlling salamander locomotion, and developing an amphibious salamander-like robot capable of replicating its bimodal locomotion, namely swimming and terrestrial walking. The controllers of the robot are central pattern generator models inspired by the salamander's locomotion control network. The goal of the project is twofold: (1) to use robots as tools for gaining a better understanding of locomotion control in vertebrates and (2) to develop new robot and control technologies for developing agile and adaptive outdoor robots. The article has four parts. We first describe the motivations behind the project. We then present neuromechanical simulation studies of locomotion control in salamanders. This is followed by a description of the current stage of the robotic developments. We conclude the article with a discussion on the usefulness of robots in neuroscience research with a special focus on locomotion control.

Index Entries: Salamander; lamprey; locomotion; gait transition; swimming; walking, simulation; robotics.

(Neuroinformatics DOI: 10.1385/NI:3:3:171)

Introduction

The ability to efficiently move and coordinate their body are key and fascinating characteristics of animals. These abilities have been shaped by millions of years of evolutionary changes and are often looked with awe by engineers. In particular, the skills to coordinate multiple degrees of freedom, using compliant actuators (muscles and tendons), and massively parallel

[*]Author to whom all correspondence and reprint requests should be addressed.
E-mail: auke.ijspeert@epfl.ch

control (the central nervous system), give animals an agility and energy efficiency not yet replicated in man-made robots. Typical examples include animal swimming compared to propelled, underwater machines, and quadruped running compared to wheeled or caterpillar-tracked machines.

The purpose of this project is to develop an amphibious robot whose structure and control are inspired by the salamander in two aspects: the biomechanical structure and the locomotion control. The first purpose of the project is to explore and develop new technologies inspired by the salamander. In particular, we aim at developing a robot that can robustly swim, crawl, and walk. The second purpose is to develop neuronal models to provide insights into salamander locomotion control and to use the robot as a test-bed for neurobiological models in a real (as opposed to simulated) embodiment. To complement the robotic project, we also carry out *neuromechanical* simulation studies, that is, simulations, which combine numerical models of the spinal neural networks controlling locomotion with a mechanical model of the salamander's body in interaction with its environment (water or ground).

Why the Salamander?

The salamander, a tetrapod capable of both swimming and walking, offers a remarkable opportunity to investigate vertebrate locomotion. First, as an amphibian with a sprawling posture and axial locomotion, it represents, among vertebrates, a key animal in the evolution from aquatic to terrestrial habitats (Cohen, 1988; Gao and Shubin, 2001). Second, the salamander has orders of magnitudes fewer neurons than mammals (Roth et al., 1993, 1997) and is therefore at a level of complexity, which is more tractable from a comprehension and modeling point of view. Finally, the central nervous system of the salamander shares many similarities with that of the lamprey, an extensively studied primitive fish, and many data and models of the lamprey's swimming circuitry are therefore available to guide the understanding of the salamander's locomotor circuitry.

From a robotics point of view, it will be very attractive to develop an amphibious robot capable of swimming, crawling, and walking. To the best of our knowledge, such a robot has never been developed before. The robot will be able to move in a large variety of environments that combine aquatic and terrestrial areas. It will be particularly adapted for inspection and exploration tasks, such as looking for survivors after an earthquake or a flood.

Related Work

Neural Control of Salamander Locomotion

There is a large amount of data available characterizing the kinematics of salamander locomotion, including axial movements (Edwards, 1976; Frolich and Biewener, 1992; Carrier, 1993; Delvolvé et al., 1997; Gillis, 1997; Ashley-Ross and Bechtel, 2004), hindlimb kinematics (Ashley-Ross, 1994a, b), and backward walking (Ashley-Ross and Lauder, 1997).

The salamander uses an anguiliform swimming gait very similar to the lamprey. The swimming is based on axial undulations in which rostrocaudal waves with a piece-wise constant wavelength are propagated along the whole body with limbs folded backwards (Fig. 1, right). As in the lamprey, the average wavelength usually corresponds to the length of the body (i.e., the body produces one complete wave) and does not vary with the frequency of oscillation (Frolich and Biewener, 1992; Delvolvé et al., 1997).

On ground, the salamander switches to a stepping gait, with the body making S-shaped standing waves with nodes at the girdles (Frolich and Biewener, 1992; Delvolvé et al., 1997). The stepping gait has the phase relation of a trot in which laterally opposed limbs are out of phase, whereas diagonally opposed limbs are in phase. The limbs are co-ordinated with the bending of the body to increase the

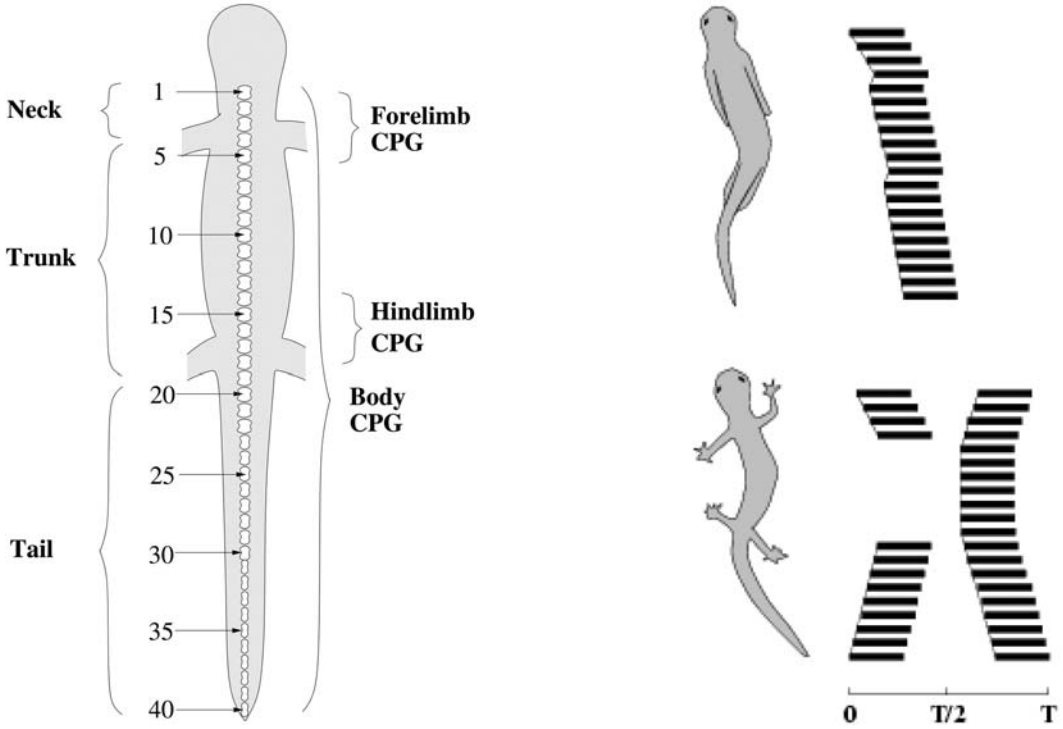

Fig. 1. Left: Schematic dorsal view of the salamander's body. Right: Patterns of EMG activity recorded from the axial musculature during swimming (top) and walking (bottom), adapted from Delvolvè et al., 1997. During swimming, a traveling wave of muscle activity is recorded (black horizontal lines). The phase lag between consecutive recording points is piecewise constant. There is a single burst per cycle. During walking, the EMG signals are more complex with double bursts in the neck and in the tail, and single bursts in the trunk. An important difference with swimming is that muscles in the trunk are active in synchrony (i.e., without phase lag) as opposed to the traveling wave observed during swimming. This correlates with the kinematics studies, which have observed traveling waves of lateral body bending during swimming and S-shaped standing waves during walking.

stride length in this sprawling gait. EMG recordings (Frolich and Biewener, 1992; Delvolvé et al., 1997) and kinematic studies (Ashley-Ross and Bechtel, 2004) have confirmed the bimodal nature of salamander locomotion, with axial travelling waves along the body for swimming and mainly standing waves coordinated with the limbs for walking (Fig. 1). Interestingly, the salamander sometimes uses crawling as a third locomotion mode, for instance when trying to rapidly escape in grass (Avis Cohen, personal communication). This crawling gait is very similar to the swimming gait on ground (i.e., with limbs folded against the body).

Locomotion of the salamander is controlled by a central pattern generator (CPG), i.e., a network of neurons capable of producing coordinated patterns of rhythmic neural activity without rhythmic inputs (Delvolvé et al., 1999). The CPG underlying axial motion—the body CPG—is located all along the spinal cord. Similarly to the lamprey (Cohen and Wallen, 1980), it spontaneously propagates traveling waves corresponding to fictive swimming when induced by NMDA excitatory baths in isolated spinal cord preparations (Delvolvé et al., 1999). Small isolated parts of two to three segments can be made to oscillate suggesting that rhythmogenesis

is similarly distributed in salamander as in the lamprey.

The neural centers for the limb movements are located within the cervical segments C1 to C5 (Fig. 1, left) for the forelimbs and within the thoracic segments 14 to 18 for the hindlimbs (Székely and Czéh, 1976; Wheatley, 1992; Cheng et al., 1998). Evidence from spinal sections (Székely and Czéh, 1976) show that these regions can be decomposed into left and right neural centers, which independently coordinate with each limb.

Finally, independent oscillatory centers for forelimb extensor and flexor motoneuron pools have been identified by electromyograph (EMG) recordings in the mudpuppy (Cheng et al., 1998). The centers are located in cervical segments C2 (elbow flexor center) and C3 (elbow extensor center), and can be made to oscillate independently with electrical and chemical stimulation. This interesting finding suggests that the walking CPG is decomposed into even smaller oscillatory units than Grillner's hypothesized "unit burst generators" for each limb and joints (Grillner, 1985).

Related Modeling Studies

To the best of our knowledge, only three previous modeling studies investigated which type of neural circuits can produce the typical swimming and walking gaits of the salamander. In Ermentrout and Kopell (1994), the production of S-shaped standing and traveling waves was mathematically investigated in a chain of coupled oscillators with long-range couplings. It is found that for a range of strengths of the long-range inhibitory coupling, an S-shaped standing wave is a stable solution. Traveling waves can also be obtained but only by changing the parameters of the coupling. In Ijspeert (2001), it was demonstrated that a leaky-integrator neural network model of a lamprey-like CPG could be extended with a limb CPG to produce stable swimming and walking gaits. Finally, in Bem et al. (2003), it was similarly demonstrated that a neural network model of the lamprey swimming controller could produce the piece-wise constant swimming of salamander and the S-shaped standing wave of walking depending on how phasic input drives (representing signals from the limb CPGs and/or sensory feedback) are applied to the body CPG. The current project extends these previous studies by investigating more systematically different potential body-limb CPGs configurations underlying salamander locomotion.

Also related to this project are models of the lamprey swimming circuitry. The lamprey is a primitive eel-like fish that swims using an anguiliform swimming gait. The network of neurons located in its spinal cord, which controls the motion has been extensively studied (Buchanan and Grillner, 1987; Grillner et al., 1988, 1991, 1995). The CPG controlling the swimming has been modeled at several levels of abstraction, namely, at a biophysical, a connectionist and an abstract oscillator level. Biophysical models using relatively realistic neural models have demonstrated that the current state of knowledge of the lamprey is sufficient to produce models whose results agree with the physiological observations (Ekeberg et al., 1991; Wallén et al., 1992). Connectionist models of the CPG (Buchanan, 1992; Williams, 1992; Ekeberg, 1993) use less realistic neuron models, which capture only the main feature of neurons, that is, their ability to change the frequency of action potential spikes in their axon (the output) depending on the sum of activity in their dendrites (the total input). These have demonstrated that the connectivity in itself is sufficient to produce many of the oscillation patterns observed in the real lamprey without the need for complicated neuronal mechanisms. Finally, at the most abstract level, the swimming controller can be modeled as a chain of mathematical oscillators in order to study which kind of couplings can produce a phase relation between segments, which is

constant over the whole spinal cord of the lamprey and also remains a fixed proportion of a cycle when the frequency of the oscillations is changed (Kopell, 1995; Williams and Sigvardt, 1995).

An important aspect of our modeling study is that we combine the neural simulations with mechanical simulations in order to investigate locomotion control in a complete loop, which includes the central nervous system, the body, and the environment. Only few simulation studies combine these aspects, interesting examples include models of lamprey (Ekeberg, 1993) and human locomotion (Taga, 1998). In our view, such a comprehensive approach is essential to correctly understand locomotion control.

Related Robotics Studies

There is quite a large number of robots inspired by animal morphology, for example, snake robots, or six-, four-, two-legged robots. There are three robots featuring an articulated spine and replicating the sprawling posture of the salamander (Lewis, 1996; Breithaupt et al., 2002; Hiraoka and Kimura, 2002). These robots are however not amphibious, and would require major changes in design to be capable of swimming. Some amphibious robots include snake- or eel-robots (McIsaac and Ostrowski, 1999; Wilbur et al., 2002; Hirose and Fukushima, 2002), a lobster robot (Ayers and Crisman, 1993), and the hexapod robot Rhex (Saranli et al., 2001). To the best of our knowledge, there is currently no amphibious robot capable of swimming, crawling, and walking.

Most articulated robots are controlled by classical methods from control theory, which use models of the robot and the environment to develop control policies for locomotion. Some methods rely on prerecorded (joint angle) trajectories, for example, such as the Zero-Moment Point (ZMP) method (Vukobratovic and Borovac, 2004), others do online trajectory generation using specific control laws, such as Virtual Model Control (Pratt et al., 2001). These methods have encountered good successes when accurate models of the robot and the environment are available, but have otherwise problems dealing with complex dynamic environments and with robots that are difficult to model accurately (e.g., compliant robots).

An alternative approach, the one taken in this project, is to develop CPG and reflex based controllers inspired by animal motor control (Taga et al., 1991; Fukuoka et al., 2003). The purpose of using CPG and reflex based control algorithms for legged robots is to obtain stable locomotion as the result from the interaction between the rhythm-generating controller, the body, and the environment. From a dynamical systems point of view, locomotion becomes the limit cycle behavior of the controller-body-environment system. Small perturbations of the system are quickly forgotten and will not destroy the cyclic movements as long as they remain within the basin of attraction of this limit cycle. The interesting aspect of this approach is that trajectories are generated online and smoothly adapt to perturbations.

Neuromechanical Simulations of Salamander Locomotion

This section describes our modeling efforts of the salamander locomotor network. We first describe the questions that we address in this study. We then describe the different components of our numerical simulations.

Questions Addressed in This Study

Despite the amount of data characterizing the salamander locomotor system, three main questions remain to be solved:

1. the neuronal basis of rhythm generation,
2. the projections (couplings) between different oscillatory centers, and
3. the mechanisms of gait transition.

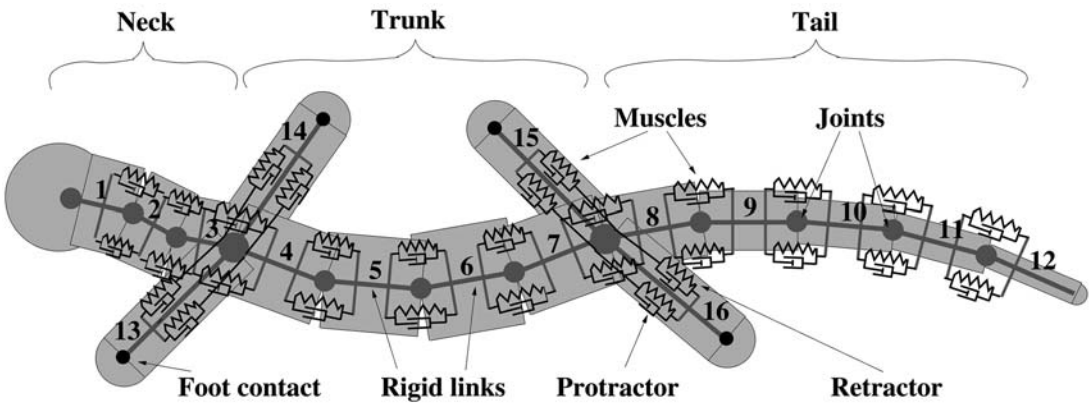

Fig. 2. Mechanical model of the salamander's body. The two-dimensional body is made of 16 rigid links connected by one-degree-of-freedom joints. Each joint is actuated by a pair of antagonist muscles simulated as springs and dampers.

In this article, we address the two last questions. In particular, we try to answer the following questions:

1. How are body and limb CPGs coupled to produce traveling waves of lateral displacement of the body during swimming and standing waves during walking?
2. How is sensory feedback integrated into the CPGs?
3. Does sensory feedback play a major role in the transition from traveling waves to standing waves?
4. To what extent is the inter-limb coordination between fore and hind limbs owing to inter-limb coupling and/or the coupling with the body CPG?

Clearly most of these questions are relevant to tetrapods in general.

Numerical Simulations

We develop computational models of the spinal circuits controlling the axial and limb musculature and investigate how these circuits are coupled to generate and switch between, the aquatic and terrestrial gaits. In previous work, one of us developed neural network models of the salamander's locomotor circuit based on the hypothesis that the circuit is constructed from a lamprey-like CPG extended by two limb CPGs (Ijspeert, 2001). In that work, a genetic algorithm was used to instantiate synaptic weights in the models to optimize the ability of the CPG to generate salamander-like swimming and walking patterns. Here, we develop models based on coupled nonlinear oscillators, and extend that work by systematically investigating different types of couplings between the oscillators capable of producing the patterns of activity observed in salamander locomotion. The use of nonlinear oscillators instead of neural network oscillators allows us to reduce the number of state variables and parameters in the models and to focus on a systematic study of the interoscillator couplings. Before describing the CPG models, we shall briefly explain the mechanical simulation.

Mechanical Simulation

The two-dimensional mechanical simulation of the salamander is an extension of Ekeberg's simulation of the lamprey (Ekeberg, 1993). The 25 cm long body is made of 12 rigid links representing the neck, trunk, and tail and four links representing the limbs (Fig. 2). The links are connected by one-degree-of-freedom joints, and the torques on each joint are determined by pairs of antagonist muscles simulated as springs and dampers. The signals sent by the

locomotion controller contract muscles by modifying (increasing) their spring constant.

The accelerations of the links are due to four types of forces: the torques owing to the muscles, inner forces linked with the mechanical constraints due to the joints, contact forces between body and limbs, and environmental forces. The environmental forces depend on whether the salamander is in water or on the ground. In water, it is assumed that each link (limb included) is subjected to inertial forces owing to the water (with forces proportional to the square of the speed of the links relative to the water). More detailed models of the hydrodynamic forces can be found in Carling et al. (1998) for lamprey swimming. On ground, all body links are subjected to a friction force, representing the fact that the trunk and the tail of the salamander slides on the ground when the salamander is trotting. As only the accelerations in the horizontal plane are calculated, we represent the contact of a limb with the ground as a friction force applied to the extremity of the limb link. We assume that the contact in itself is determined by the signals sent to the horizontal protractor and retractor muscles. The limb is assumed to be in the air (i.e., without friction) when the signal of the protractor is larger than that of the retractor, and on the ground otherwise. The motoneurons for the retractor and protractor therefore not only determine the torque of the limb, but also its stance and swing phases. The mechanical simulation is described in more detail by Ijspeert (2001).

The simulation is written in C (approx 1500 lines of code), and uses a fourth order Runge–Kutta algorithm for integrating the differential equations. The integration step size is 1 ms. At every integration step, it receives signals from the locomotion controller that determine the contraction of the simulated muscles and returns the states of joint angles for computing the sensory feedback signals from stretch receptors (*see* next section). The simulation includes a 3D visualization environment based on OpenGL (approx 2000 lines of code). Useful quantities that can be measured in the simulation include the speed of locomotion, the time evolution of the body shape (e.g., joint angles and lateral displacements), and the used mechanical energy.

Locomotion Controller

Nonlinear Oscillator

The building block of our model of the CPGs is the following nonlinear oscillator:

$$\tau \dot{\nu} = -\alpha \frac{x^2 + \nu^2 - E}{E} \nu - x \tag{1}$$

$$\tau \dot{x} = \nu \tag{2}$$

where τ, α, and E are positive constants. This oscillator has the interesting property that its limit cycle behavior is a sinusoidal signal with amplitude $\sqrt{E}$ and period $2\pi\tau$. The state variable $x(t)$ indeed converges to $\tilde{x}(t) = \sqrt{E}\ sin(t/\tau + \phi)$ where ϕ depends on the initial conditions, *see* also Fig. 3.

We assume that the different oscillators of the CPG are coupled together by projecting to each other signals proportional to their x and v states in the following manner:

$$\tau \dot{\nu}_i = -\alpha \frac{x_i^2 + \nu_i^2 - E_i}{E_i} \nu_i - x_i + \sum_j (a_{ij} x_j + b_{ij} \nu_j) + \sum_j c_{ij} s_j \tag{3}$$

$$\tau \dot{x}_i = \nu_i \tag{4}$$

where a_{ij} and b_{ij} are constants (positive or negative) determining how oscillator j influences oscillator i. In these equations, the influence from sensory inputs s_j weighted by a constant c_{ij} is also added. The number of oscillators, their couplings, and the type of sensory feedback will be explained in the next sections.

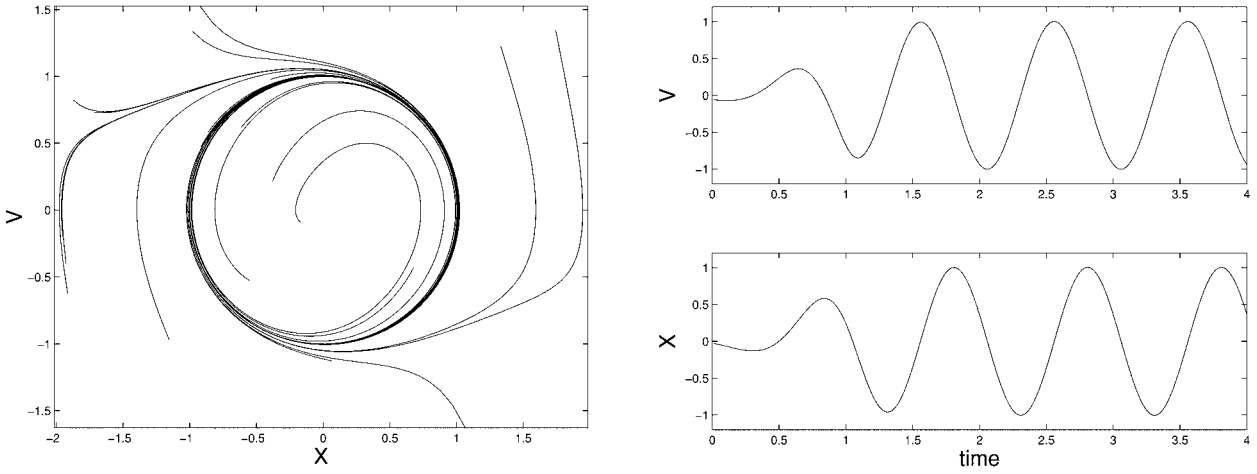

Fig. 3. Limit cycle behavior. Left: phase plot of the time evolution of the nonlinear oscillator with different random initial conditions. Right: particular example of the time evolution of *x* and *v*.

The simulation is written in C (approx 1000 lines of code), and uses a first order Euler algorithm for integrating the differential equations. The integration step size is 1 ms. Useful quantities that can be measured include the state variables of all oscillators, the period and amplitude of oscillations, and the time required for reaching the limit cycle behavior.

Body CPG

We assume that the body CPG is composed of a double chain of oscillators all along the 40 segments of spinal cord. The types of connections investigated in this article are illustrated in Fig. 4 (left). For simplicity, we assume that only nearest neighbor connections exist between oscillators. In our first investigation, the oscillators are assumed to be identical along the chain (with identical projections), as well as between each side of the body. The connectivity of the chain is therefore defined by six parameters, two parameters (a_{ij} and b_{ij}) for the three types of projections from one oscillator to the other (i.e., the rostral, caudal, and contralateral projections). Of these six parameters, we fixed the couplings between contralateral oscillators to $a_{ij} = 0$ and $b_{ij} = -0.5$ in order to force them to oscillate in antiphase. We systematically investigated the different combinations of the four remaining parameters (the rostral and caudal projections) with values ranging from –1.0 to 1.0, with a 0.1 step.

Traveling Wave Experiments on isolated spinal cords of the salamander suggest that, similarly to the lamprey, the body CPG tends to propagate rostro-caudal (from head to tail) traveling waves of neural activity (Delvolvé et al., 1999). During (intact) swimming, the wavelength of the wave corresponds approximately to a bodylength. We therefore systematically investigated the parameter space of the body CPG configuration to identify sets of parameters leading to stable oscillations with phase lags between consecutive segments approximately equal to 2.5% of the period (in order to obtain a 100% phase lag between head and tail). The goal is to obtain traveling waves that are due to asymmetries of interoscillator coupling, while maintaining the same intrinsic period (the same τ) for all oscillators.

We found that several coupling schemes could lead to such traveling waves. The coupling schemes can qualitatively be grouped in three different categories: dominantly caudal couplings, balanced caudal and rostral

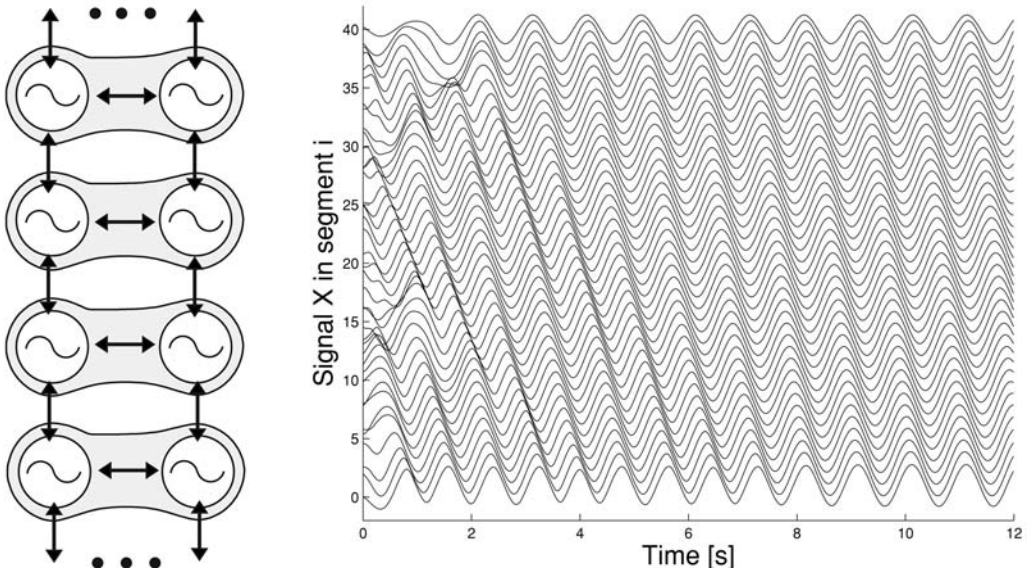

Fig. 4. Left: Configuration of the body CPG. Right: oscillations in a 40-segment chain (only the activity on one side of the body is shown).

couplings, and dominantly rostral couplings.[1] By dominant, we mean that the sum of the absolute values of the weights in one direction is significantly larger than that in the other direction. Whereas all groups can produce traveling waves corresponding to salamander swimming, solutions that have balanced caudal and rostral couplings need significantly more cycles to stabilize into the traveling wave (starting from random initial conditions) than the solutions in which one type of coupling is dominant. Since the traveling waves of salamander swimming stabilize very quickly, it is therefore likely that the salamander has one type of coupling, which is dominant compared to the other. A very similar conclusion has been made concerning the lamprey swimming controller (Kopell, 1995). But note that intersegmental coupling in the lamprey is known to be significantly more complex than the nearest neighbor coupling assumed here, with both short and long range projections of different strengths (Kiemel et al., 2003). Below we will argue that it is most likely that, in the salamander, the rostral coupling is dominant.

Figure 4 (right) illustrates the traveling waves generated by one of the dominantly caudal chains. As can be observed, starting from random initial states, the oscillations rapidly evolve to a traveling wave. Since the period of the oscillations explicitly depend on the parameter τ, the period can be modified independently of the wavelength. The wavelength of one-body length is therefore maintained for any period, when all oscillators have the same value of τ (i.e., the same intrinsic period). This allows one to modify the speed of swimming by only changing the period of oscillation, as observed in normal lamprey and salamander swimming.

[1]Dominantly caudal and rostral couplings are essentially equivalent since each coupling type that is dominant in one direction has an equivalent in the other direction by inverting the sign of the a_{ij} weights. However, that equivalence is lost when the intrinsic frequencies of some oscillators are varied, *see* the "Piece-wise constant wavelength" paragraph.

Interestingly, although the connectivity of the oscillators favors a one-body length wavelength, it is possible to vary the wavelength by modifying the intrinsic period of some oscillators, those closest to the head, for instance. In the real neural network, a change of oscillation period can be obtained by locally increasing or reducing the tonic drive to a segmental oscillator. Reducing the period of these oscillators leads to an increase of the phase lag between consecutive oscillators (a reduction of the wavelength), whereas increasing their period leads to a decrease of the phase lag and can even change the direction of the wave (i.e., generate a caudo-rostral wave). This type of behavior is typical of chains of oscillators (Kopell, 1995).

Piece-Wise Constant Wavelength We identify at least four potential causes for the small changes of wavelength observed along the body at the level of the girdles:

1. differences of intrinsic frequencies between the oscillators at the girdles and the other body oscillators (e.g., owing to the limb oscillators),
2. differences in intersegmental coupling along the body CPG (with three regions: neck, trunk, and tail),
3. effect of the coupling from the limb CPG,
4. effect of sensory feedback.

Recent in vitro recordings on isolated spinal cords showed that a local change of wavelength along the cord is also observed during fictive swimming (unpublished data). Therefore it seems that the phenomenon is mainly owing to the CPG configuration rather than to sensory feedback (explanation number four is therefore less likely). We tested these different hypotheses with the numerical simulations. For the hypothesis two, it meant adding eight parameters for differentiating the intersegmental couplings in the neck, trunk, and tail regions.

The results suggest that, in our framework, the most likely cause of the three-wave pattern is a combination of differences in intersegmental coupling and of intrinsic frequencies of oscillators at the girdles. The differences in intersegmental coupling lead to variations in the wavelength of the undulation along the spinal cord, but they do not explain the abrupt changes of phases at the level of girdles. These are best explained by small differences in intrinsic frequencies of oscillators of the body CPGs at the two girdles (these could also potentially be owing to the projections from the limb CPG, *see* the following sections).

We can furthermore tell that the effect of variations of the intrinsic frequencies depend on which coupling is dominant in the body CPG. The patterns observed in the salamander are best explained with either a combination of dominantly caudal coupling and higher intrinsic frequency at the girdles, or dominantly rostral coupling and lower intrinsic frequencies at the girdles. The resulting activity in the latter configuration is illustrated in Fig. 5 (top). Since limb oscillators at the girdles tend to oscillate at lower frequencies than the body oscillations during swimming (walking frequencies are indeed systematically lower than swimming frequencies [Delvolvé et al., 1997]), we believe that it is most likely that the body CPG of the salamander is organized with a coupling that is dominant in the rostral direction. This is in agreement with several studies in the lamprey, suggesting an ascending bias in the intersegmental coupling (Williams, et al., 1990; Williams and Sigvardt, 1994; Kiemel et al., 2003).

Swimming We tested the body CPG in the mechanical simulation for controlling swimming. Since the mechanical simulation has only 11 joints along the body, 11 pairs of equally spaced oscillators were picked from the body CPG to drive the muscle models, such that the oscillators in one pair project to the muscle on their respective side. A

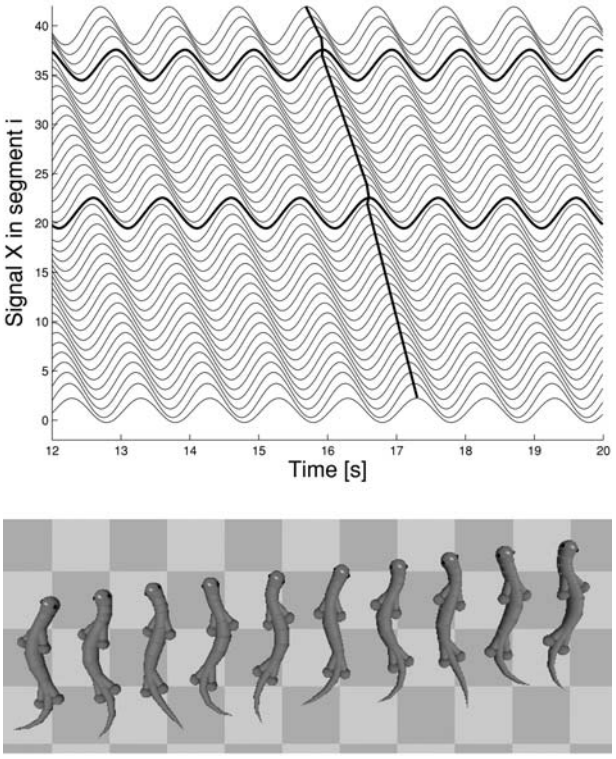

Fig. 5. Swimming gait. Top: Piece-wise constant wavelength. The oscillations at the level of the girdles are drawn with thicker lines. Bottom: resulting swimming behavior (in steady state).

"motoneuron" m_i signal is obtained from the states x_i with the equation $m_i = \beta\max(x_i,0)$, where β is a positive constant gain. This motoneuron signal controls how much a muscle contracts by essentially changing the spring constant of the spring and damper muscle model see the work of Ijspeert (2001). An example of the swimming gait is shown in Fig. 5 (bottom). The speed of swimming can be modulated by changing the frequency of all oscillators (through the parameter τ), whereas the direction of swimming can be modulated by applying an asymmetry of the amplitude parameter E between left and right sides of the chain. The salamander will then turn toward the side receives the highest amplitude parameter.

Different Body-Limb CPG Configurations for Gait Transition

One of the goals of this article is to investigate different types of couplings between the body and limb CPGs, and how these couplings affect the gait transitions between swimming and walking. There are currently too few biological data available to indicate how the different neural oscillators in the body and limb CPGs are interconnected. Our aim is to investigate which of these configurations can best reproduce some key characteristics of salamander locomotion.

We tested five different types of coupling (Fig. 6). These couplings differ in three characteristics: *unidirectional/bidirectional* couplings in which the limb CPGs are either unidirectionally or bidirectionally (i.e., in both directions) coupled to the body CPG, *global/local* couplings in which the limb CPGs project either to many body CPG oscillators, or only to those close to the girdles and *with/without* interlimb couplings between fore- and hindlimbs. In our previous work (Ijspeert, 2001), we tested configuration A (unidirectional, global, with interlimb coupling) using neural network oscillators. The unidirectional projections from limb to body CPG essentially mean a hierarchical structure in the CPG for that configuration. Note that we did not study all possible combinations without interlimb couplings (only a single one, configuration E) in order to reduce the number of configurations to test.

In all configurations, we assume that two different control pathways exist for the body and the limb CPGs, in other words, that the control parameters τ and E can be modulated independently for the body and limb oscillators. In particular, we make the hypothesis that the gait transition is obtained as follows: swimming is generated when *only* the body CPG is activated ($E_{body} = 1.0$ and $E_{limb} = 0.005$), and walking is generated when *both* body *and* limb CPGs are activated ($E_{body} = 1.0$ and $E_{limb} = 1.0$). The small

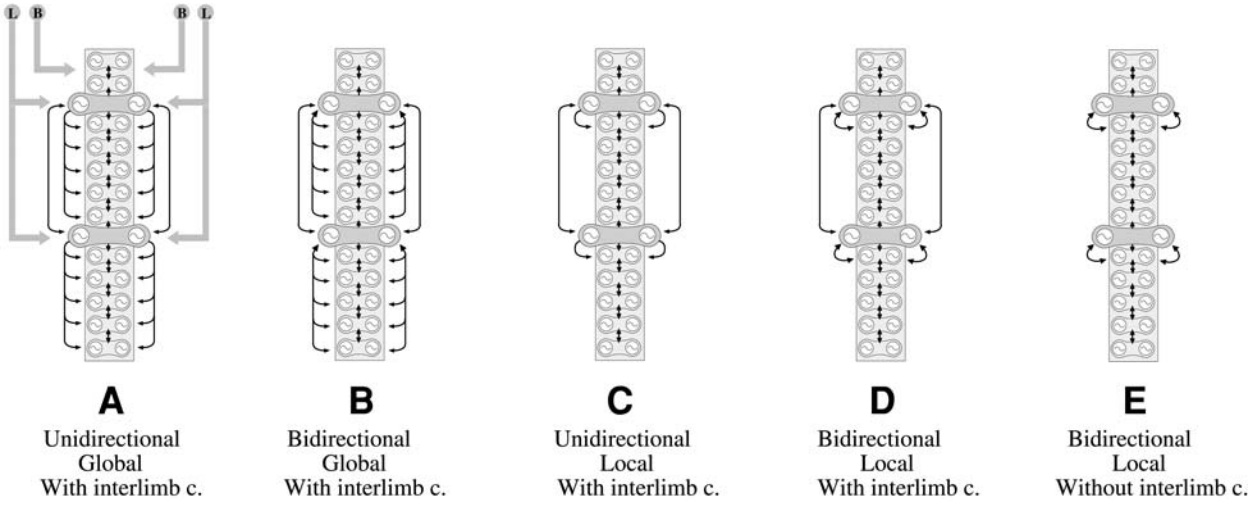

Fig. 6. Different potential CPG configurations.

Elimb value during swimming means that the limb oscillators are almost silent (they have a very small amplitude), and that their influence on the body oscillators are negligible.

The simulation results show that only configurations A and B, i.e., those with global coupling between limb and body CPG can produce standing waves (in the absence of sensory feedback). For these configurations, the global coupling from limb oscillators to body oscillators ensures that the body CPG oscillates approximately in synchrony in the trunk and in the tail when the limb CPG is activated (Fig. 7). For the other configurations (C, D, and E) the fact that the couplings between limb and body CPGs are only local means that traveling waves are still propagated in the trunk and the tail, despite the influence from the limb oscillators. Configuration E, which lacks interlimb couplings can still produce walking gaits very similar to those of configurations C and D, because the coupling with the body CPG gives a phase relation between fore- and hindlimbs of approx 50% of the period (because fore- and hindlimbs are separated by approximately half of one body-length).

Having bidirectional couplings between limb and body CPGs does not affect the walking pattern in a significant way. However, if the coupling from body CPG to limb CPG is strong, it will affect the swimming gait. In that case, even if the amplitude of the limb oscillators is set to a negligible value (E_{limb} = 0.005), the inputs from the body CPG will be sufficient to drive the limb oscillators, which in return will force the body CPG to generate a wave, which is a mix between a traveling wave and standing wave. It is therefore likely that the couplings between limb and body CPG are stronger from limb to body CPG than in the opposite direction.

Note the fact that CPG configurations C, D, and E cannot produce standing waves, does however not exclude the possibility that these configurations produce standing waves when sensory feedback is added to the controller. This will be investigated in the next section.

Effect of Sensory Feedback When a lamprey is taken out of the water and placed on ground, it tends to make undulations that look almost like standing waves because the lateral displacements do not increase along the body but form quasi-nodes (i.e., points with very little lateral displacements) at some points along the body (Bowtell and Williams, 1991).

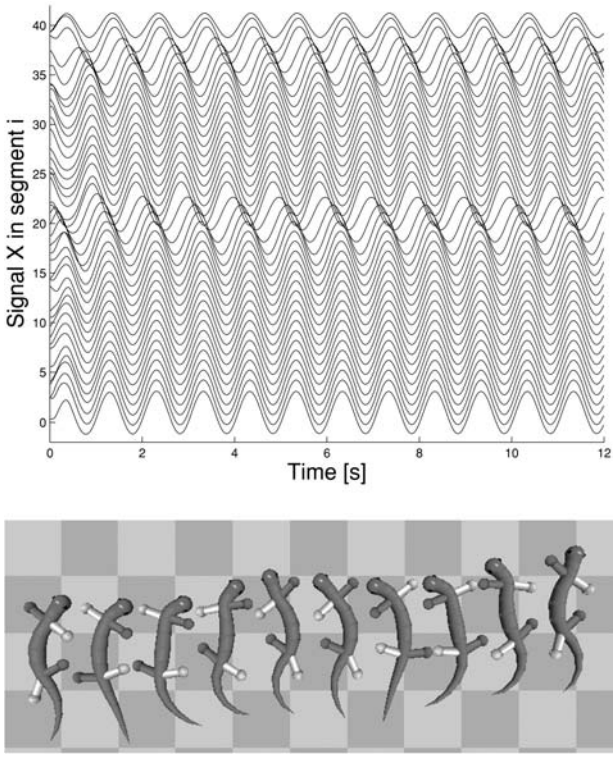

Fig. 7. Walking gait. Top: oscillations along the body in a CPG of type A (only the activity on one side of the body is shown). Bottom: resulting walking behavior (in steady state).

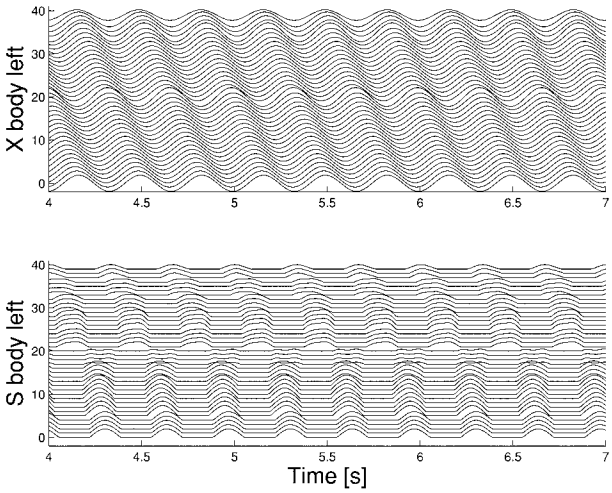

Fig. 8. Walking gait produced by configuration D, without sensory feedback. Top: output of the body CPG, Bottom: output of the stretch sensors.

Interestingly, the same is true in our simulation. When the swimming gait is used on ground (without sensory feedback), the body makes an S-shaped standing wave undulation instead of the traveling wave undulation generated in water. This is because of the differences between hydrodynamic forces in water (which have strongly different components between directions parallel and perpendicular to the body) and the friction forces on ground (which are uniform). The sensory signals from such a gait are then reflecting this S-shaped standing wave, despite the traveling waves sent to the muscles.

The fact that such sensory feedback on ground exhibits S-shaped standing waves means that sensory feedback could provide a potential explanation for the transition from a traveling wave for swimming to a standing wave for walking. We therefore tested the effect of incorporating sensory feedback in the different CPG configurations described above. Sensory feedback to the salamander's CPG is provided by sensory receptors in joints and muscles (Ottoson, 1976). Intraspinal edge cells, similar to those of lamprey (e.g., McClellan and Sigvardt, 1988; Viana Di Prisco et al., 1990) have also been identified in salamanders, but their role as stretch sensitive sensors remain to be demonstrated (Schroeder and Egar, 1990). We designed an abstract model of sensory feedback by including sensory units located on both sides of each joint, which produce a signal proportional to how much that side is stretched: $s_i = \max(\phi_i, 0)$ where ϕ_i is the angle of joint i measured positively away from the sensory unit (*see* Eq. 3). For simplicity, we only consider sensory feedback in the body segments (i.e., not in the limbs), and assume that a sensory unit for a specific joint is coupled only locally to the two (antagonist) oscillators activating that joint.

Figure 8 shows the activity of the body CPG and the sensor units produced during a stepping gait with a controller with configuration

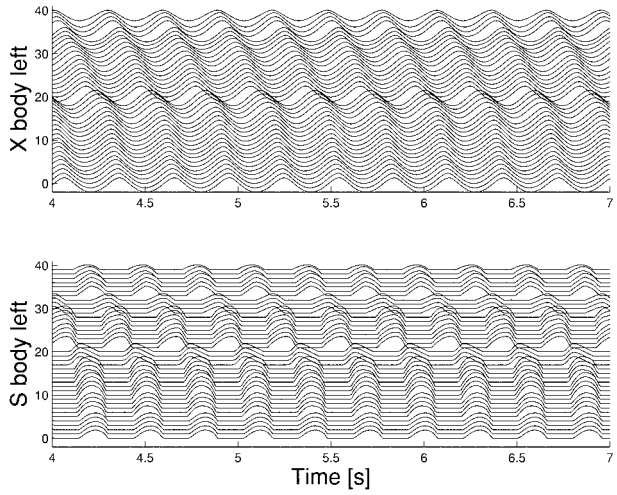

Fig. 9. Walking gait produced by configuration D, with sensory feedback. Top: output of the body CPG, Bottom: output of the stretch sensors.

D. Without sensory feedback (Fig. 8), this controller produces a traveling wave during walking because the limb oscillators have only local projections to the body CPG. Despite this traveling wave of muscular activity, the body (in contact with the ground) makes essentially an S-shaped standing wave as illustrated by the sensory signals (synchrony in the trunk and in the tail, with an abrupt change of phase in between). When these sensory signals are fed back into the CPG (Fig. 9), the body CPG activity is modified to approach the standing wave (i.e., the phase lag between segments decrease in the trunk and in particular in the tail). This illustrates that sensory feedback could indeed play a role in the production of the standing wave in the body CPG. Note that if the sensory feedback signals are too strong, the stepping gait becomes irregular. Interestingly, the sensory feedback leads to an increase in the oscillation's frequency, something, which has also been observed in a comparison between swimming with and without sensory feedback in the lamprey (Guan et al., 2001) and in the salamander (Delvolvé et al., 1999).

Discussion of the Simulation Results

The primary goal of this simulation study was to investigate which of the different CPG configurations were most likely to control salamander locomotion.

The simulation results presented in this article suggest that CPG configurations, which have global couplings from limb to body CPGs, and interlimb couplings (configurations A or B) are the most likely in the salamander. These configurations can indeed produce stable swimming and walking gaits with all the characteristics of salamander locomotion. Our investigation does not exclude the other configurations, but suggest that these would need a significant input from sensory feedback to force the body CPG to produce the S-shaped standing wave along the body. These results suggest new neurophysiological experiments. It would, for instance, be interesting to try to induce not only fictive swimming like by Delvolvé et al. (1999), but also fictive walking (e.g., by stimulation of the MLR region in the brainstem, *see* Cabelguen et al. [2003]) in an in vitro preparation. This should determine whether the activity of the body CPG during fictive walking is a standing wave (corresponding to configuration A or B) or a traveling wave (configuration C, D, or E). Additionally, tracing studies are currently under way to have an idea of the lengths of couplings between the different oscillators in the body and limb CPGs.

Note that the simulated salamander is not capable of moving forward when crawling with a serpentine gait on ground (i.e., when producing a traveling wave like swimming on ground). This is unlike the escape behavior observed in salamanders on grass. The most likely explanation for this is that grass is a medium that provides asymmetric friction forces, with forces perpendicular to each body segment being larger than the parallel ones (like water and unlike a flat ground).

The speed, direction, and type of gait in the simulation are completely controlled by simple command signals determining the amplitude and period of the oscillators, with two independent pathways, one for the body CPG oscillators and one for the limb CPG oscillators *see* Fig. 6, (left). These command signals correspond to signals that in vertebrate animals are sent from upper parts of the brain to the spinal cord via the reticular nuclei in the brainstem. In our simulation, adjusting the time parameter τ of all oscillators allows us to change the speed of locomotion (both for swimming and for walking). By modifying the amplitude parameter E for the limb oscillators, we can switch between swimming and walking, and by modifying the amplitude parameter E independently between oscillators on the left and right side of the body CPG we can control the direction (the salamander will turn to the side with the highest amplitude parameter, both for swimming and for walking). This type of control replicates how simple signals are known to initiate locomotion and to modulate the speed and direction in vertebrate animals. *See* Deliagina et al. (2000) for a nice study of the reticulospinal system during swimming in the lamprey.

To make our investigation tractable, we made several simplifying assumptions. First of all, we base our investigation on nonlinear oscillators. Clearly, these are only very abstract models of oscillatory neural networks. In particular, they have only a few state variables and fail to encapsulate all the rich dynamics produced by cellular and network properties of real neural networks. We however believe that they are well suited for investigating the general structure of the locomotion controller. To some extent, some properties of interoscillator couplings are universal and do not depend on the exact implementation of the oscillators. This is observed for instance in chains (Kopell, 1995), as well as rings of oscillators (Collins and Richmond, 1994). Our goal was therefore to analyze these general properties of systems of coupled oscillators.

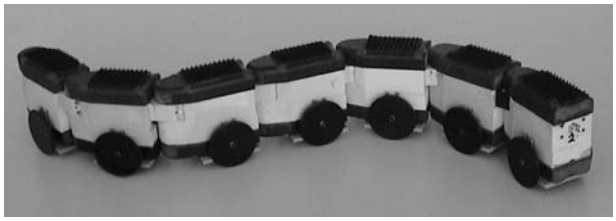

Fig. 10. The amphibious snake robot Amphibot I with passive wheels.

An interesting aspect of this work was to combine a model of the controller and of the body, since this allowed us to investigate the mechanisms of entrainment between the CPG, the body and the environment. We believe, such an approach is essential to get a complete understanding of locomotion control, since the complete loop can generate dynamics that are difficult to predict by investigating the controller (the central nervous system) in isolation of the body. The transformation of traveling waves of muscular activity into standing waves of movements when the salamander is placed on ground is an illustration of the complex dynamics that can result from the complete loop.

Robotic Developments

Based on the simulation studies, we are designing and constructing a salamander-like robot. One of the aims is to test whether the CPG models presented in the previous part could be adapted to control a real device (in addition to a physics-based simulation of the body). At the current stage an amphibious snake (or lamprey) robot called *Amphibot I* has been developed and tested (Fig. 10). The robot is capable of anguiliform swimming (like the lamprey and the salamander), and of crawling on ground using a serpentine gait (like many snake species). The Amphibot robot will serve as spine for the salamander robot (Fig. 11).

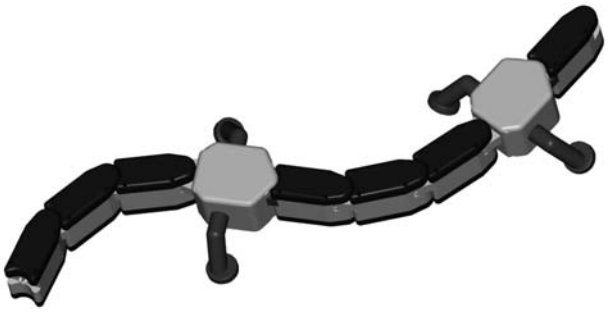

Fig. 11. Schematic view of the salamander robot currently under construction.

Design Considerations

The amphibious snake robot (Fig. 10) has been designed to be modular. It is composed of an adjustable number of identical segments (called *elements*). In this article, we worked with a seven-element robot. The main characteristics of the elements are as follows:

- *Waterproofness*: each element is waterproof (as opposed to have a coating of the complete robot), so that if there is a leakage, only the concerned element is affected and not the whole robot.
- *Independency*: each element has its own power source (battery), motor, and local motor controller.
- *Buoyancy*: the density of an element is close to that of water. Currently it is slightly higher, but we are making small modifications to make it slightly lower than the density of the water, allowing the robot to swim under the water's surface and not to sink in case of failure.
- *Vertical stability*: the center of mass of an element is slightly under the vertical center, so that the robot keeps a stable vertical orientation in water and avoids acquiring a constant angular velocity, which would produce a helicoidal motion.
- *Differential friction coefficients* on the ground: to move using serpentine locomotion, the robot needs to have a lower friction coefficient in the parallel axis compared to the perpendicular one. This is achieved with passive wheels in this article.

This kind of design has many advantages, particularly in terms of reliability, scalability and fault tolerance.

Hardware

Mechanical Description

The structure of each element is composed of four main parts, molded in polyurethane lightened with phenol microballs: the main body, the top cover, the bottom cover (which contains the battery), and the connection piece. An element has a length of 7 cm and a section of 5.5 (height) by 3.3 (width) cm, including the covers and the connection piece. To ensure the waterproofness, an O-ring is placed between each cover and the body.

The motor drives a set of reduction gears, located in the bottom part of the body, which has a reduction factor of approx 400. The last gear constitutes the output axis of an element and contains the wires needed to create an electrical connection between the elements. An O-ring ensures the waterproofness of the output axis. Fixed to the output axis is a piece providing electrical and mechanical connections to the next element. The motor has an integrated magnetic incremental encoder generating 16 pulses per turn, thus allowing a precise determination of the position of the output axis. A potentiometer fixed to the output axis provides an absolute position reference that can be used, for example, when powering the robot.

Electrical Description

Five wires pass all along the robot, one of which is currently unused. Two wires are used by the I^2C bus, the third is the ground (common to the power and the bus), and the fourth is the optional external power source, mainly used to charge the batteries. Inside each element are two double-sided printed circuits. The main elements of the first one are a power switch (for switching between battery and external power), a step-up converter to

generate 5 V for the microcontroller when the circuit is powered by the 3.6 V Li-Ion battery, and a battery charger.

The core of the second circuit is a PIC microcontroller, containing a DC motor controller code proportional integral differential (PID) developed at the Autonomous Systems Laboratory (ASL) of the EPFL. The PIC drives a low voltage H-bridge connected to the 0.75 W DC motor, and receives inputs from a quadrature detector (which filters and decodes the signals coming from the incremental encoder on the motor) and from an operational amplifier, which allows a measure of the voltage drop on a 0.2 Ω resistor inserted between the H-bridge and the motor, thus allowing an indirect measurement of the motor's torque. The parameters of the motor controller (i.e., current position, setpoint, PID factors, etc.) can be read and written over the I_2C bus (each PIC has its own address programmed in the internal EEPROM memory). The I_2C bus is currently connected to an external PC using a RS-232 $\leftrightarrow I_2C$ interface. A bidirectional wireless link is currently under development, and on-board trajectory generation is planned. For more details concerning the robot, *see* Crespi et al. (2005b).

Control of Locomotion

Controlling the locomotion of the robot requires the generation of joint-angle trajectories for its multiple degrees of freedom. A PID feedback controller is then in charge of generating the torques necessary to follow those trajectories. We tested two types of locomotion controllers: a "naive" sine-based controller and a CPG-based controller similar to the one presented in the previous section. For the moment, only swimming and crawling gaits are considered.

Sine-Based Controller

The sine-based controller sends the following setpoints (desired angles) *xi(t)* to the robot at time *t* for the *i*th joint:

$$x_i(t) = x_0 + A \cdot \sin(2\pi \cdot \upsilon \cdot t + 2\pi \cdot \Delta\phi \cdot (i-1)) \quad (5)$$

where the sinusoidal crawling or swimming gaits are characterized by the amplitude A, the frequency υ and the phase lag $\Delta\phi$. For more clarity, we use the total phase lag between head and tail $N\Delta\phi$ (i.e., the inverse of the wavelength) as a measure of the phase lag, where N is the number of active joints in the robot, so that our measure of phase is independent of the number of joints. An undulation with $N\Delta\phi = 1.0$ corresponds to an undulation in which the body makes a complete wave.

CPG-Based Controller

The CPG-based controller corresponds to the body CPG presented in subsection "Body CPG". The only differences are that the chain is made of a single oscillator per segment (instead of two), that it has a length of six segments (instead of 40), that the state variable x directly encodes a joint angle (rather than the contraction of a muscle model), and that each oscillator has an offset x_0 around which it oscillates. This offset is introduced to allow an easy control of the direction of motion.

The setpoints $xi(t)$ are computed by integrating the following differential equations:

$$\tau \dot{\nu}_i = -\alpha \frac{(x_i - x_0)^2 + \nu_i^2 - E_i}{E_i} \nu_i - (x_i - x_0) \sum_j (a_{ij}(x_j - x_0) + b_{ij}\nu_j) \quad (6)$$

$$\tau \dot{x}_i = \nu_i \quad (7)$$

Swimming and Crawling

Both the sine-based and the CPG-based controllers are capable of producing swimming and crawling gaits. Figures 12 and 13 illustrate gaits obtained with the two different media. Using the sine-based controllers, we systematically explored (in Crespi et al., 2005a) which undulations lead to the fastest gaits. We systematically varied the frequency, phase lag and

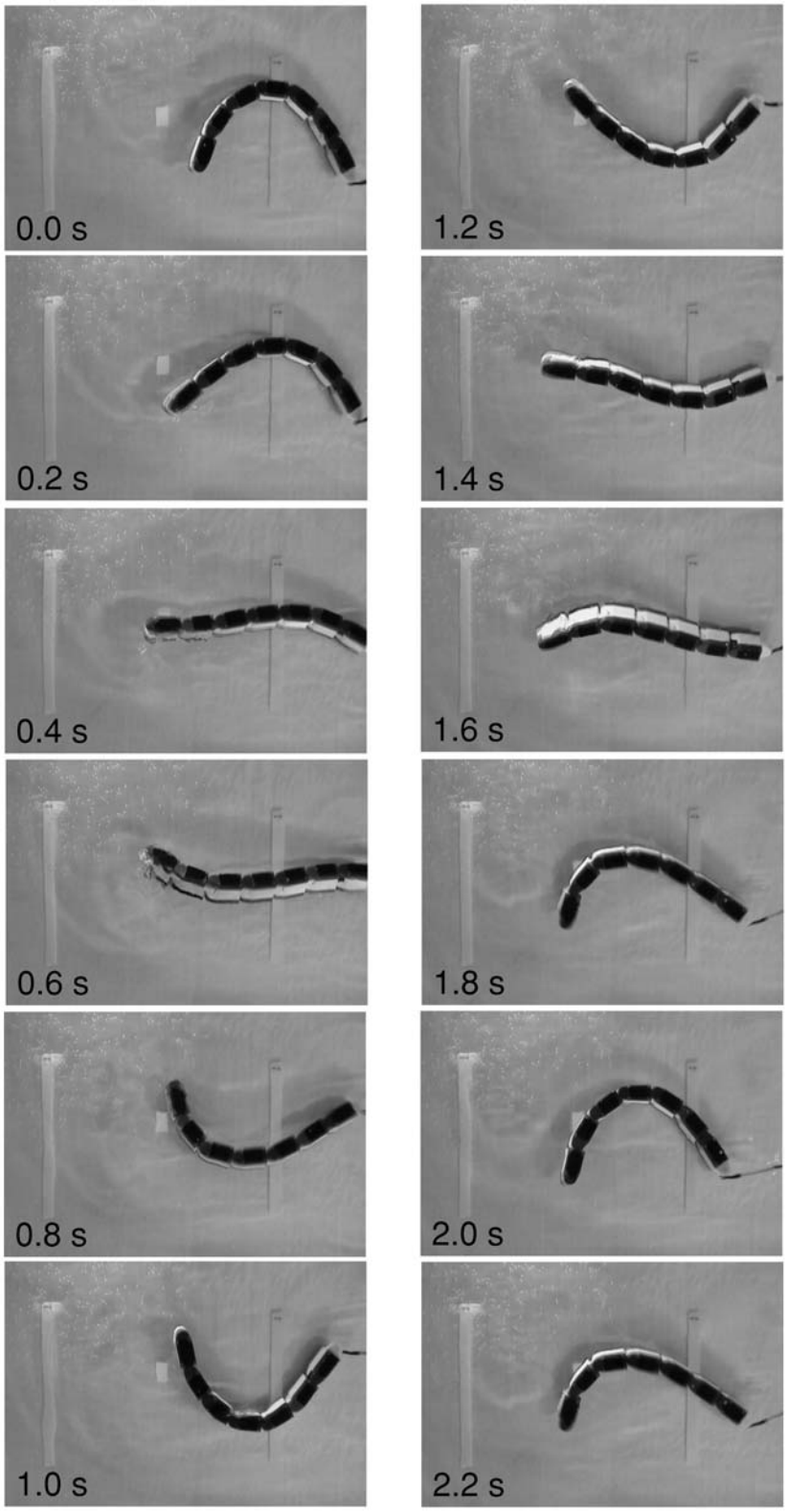

Fig. 12. The robot swimming in water with the sine-based controller (A = 40°, $N\Delta\phi$ = 0.25 and υ = 0.5 Hz).

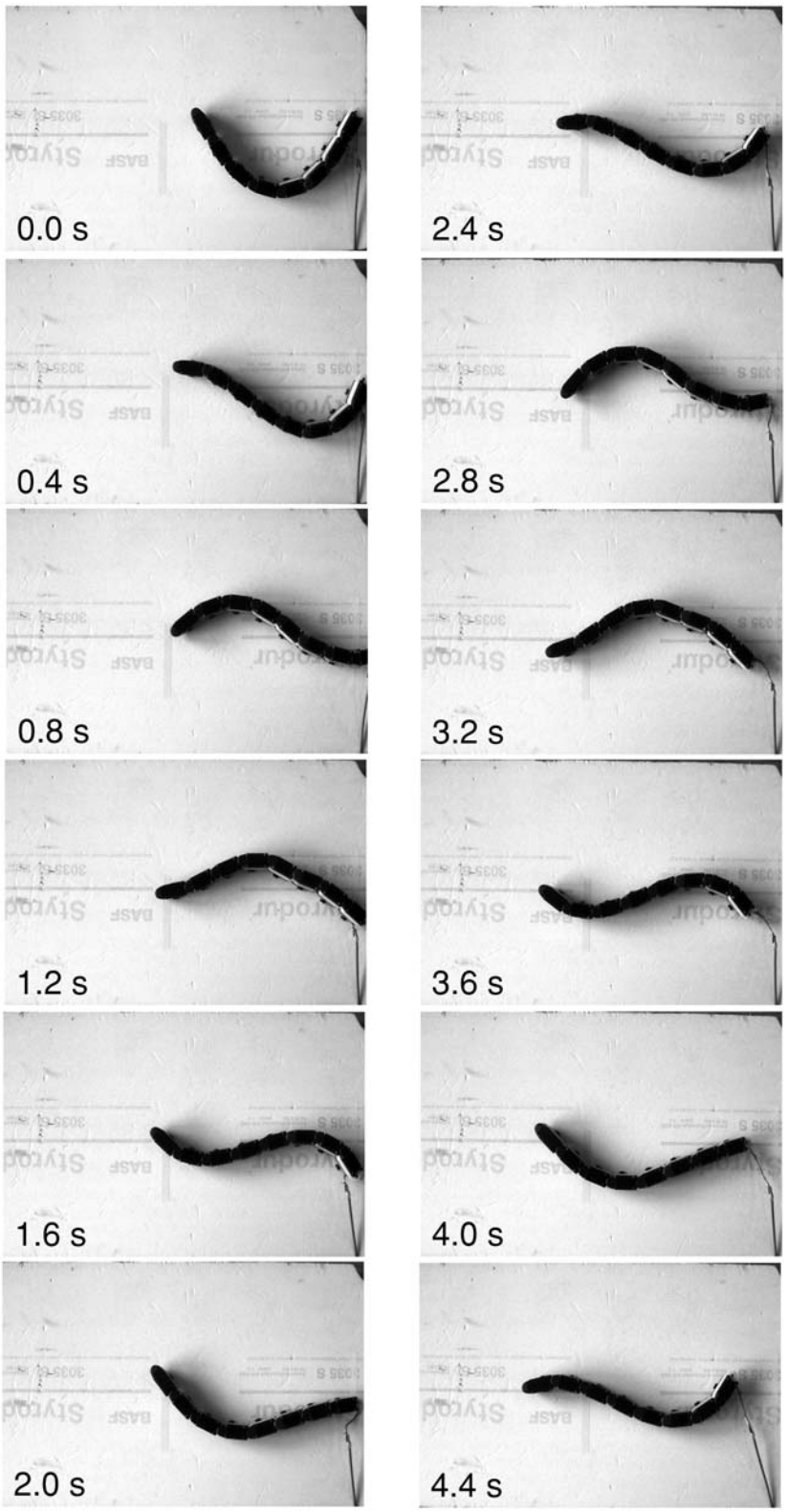

Fig. 13. The robot crawling on ground with the sine-based controller (A = 30°, $N\Delta\phi$ = 0.5 and υ = 0.5 Hz).

amplitude of the oscillations in the following ranges: $A \in [10; 15; 20; 25; 30; 35; 40]$ (degrees), $N \cdot \Delta\phi \in [0.25; 0.5; 0.75; 1.0; 1.25; 1.5]$, and $\upsilon \in [0.25; 0.5; 0.75]$ (Hz). The maxima of these ranges correspond to the current hardware limits of our robot. We found that the fastest gaits are different from one medium to the other, with larger optimal regions in parameter space for the crawling gaits. Swimming gaits are faster than crawling gaits for the same frequencies. For both media, the fastest locomotion is obtained with total phase lags that are smaller than one ($N\Delta\phi = 0{:}25$ for swimming and $N\Delta\phi = 0{:}5$ for crawling). In other words, this corresponds to undulations in which body makes a traveling C-shape, rather than a traveling S-shape as usually observed in salamander and lamprey swimming. Possible explanations of this difference include (1) the fact that the robot swims at lower frequencies (maximum of 0.75 Hz) than salamanders (often above 3 Hz), and (2) that the criterion that salamander optimizes when swimming does not correspond to the maximum speed but to something else such as maximal energy efficiency, for instance. We are currently exploring these issues further.

Although sine-based controllers are capable of controlling steady-state locomotion, they are not well suited for nonsteady state conditions such as changes of frequency or amplitude of the undulations. Figure 14 illustrates how sine-based and CPG-based controllers react when parameters encoding period of oscillations, amplitude, phase lag, and offset are abruptly varied. With the sine-based controller, abrupt changes of parameters lead to abrupt modifications of the setpoints. This leads to violent jerks, which prevent smooth locomotion and could lead to damage in the motors and gearboxes. Unlike the sine-based controller, the CPG-based controller provides smooth trajectories despite the abrupt parameter changes. This is due to the fact that trajectories are computed online by integrating the second order differential equations. One could try to design interpolation algorithms and/or filters to smoothen out the jerks owing to the sine-based controller, but that would arguably be less elegant and potentially less computationally efficient than the CPG-based controller.

Another important advantage of the CPG-based controller over the sine-based controller is that it can easily integrate feedback terms to modify the generated trajectories depending on perceptual inputs. For instance, signals from simulated stretch receptors (as discussed in the previous section) or signals proportional to the error between desired and actual joint angles can be fed back into the differential equations in order to modify trajectories accordingly. Examples of the latter type of feedback for a slightly different system applied to the control of a humanoid robot can be found in Ijspeert et al. (2002, 2003).

Discussion: Robots as Tools for Neuroscience Research

To conclude this article, we shall discuss the benefits and difficulties of using robots as tools for neuroscience research. We focus our discussion on the use of robots for testing models of motor control systems. For more general discussions on the usefulness of robots to study biological systems *see* Webb (2001, 2002).

An interesting aspect of using robots in computational neuroscience is that they allow computational models to be tested as they are coupled to a real body and embedded in a real environment. In particular, this means that models can be tested within a complete sensing to acting loop. This is important since some aspects of locomotion might depend critically on the interaction with the environment. For instance, the potential role of interaction forces and sensory feedback in gait transitions discussed in the modeling section would be difficult to study in isolated neural network models.

Dynamic simulators can be used to simulate the physics of the body and the environment,

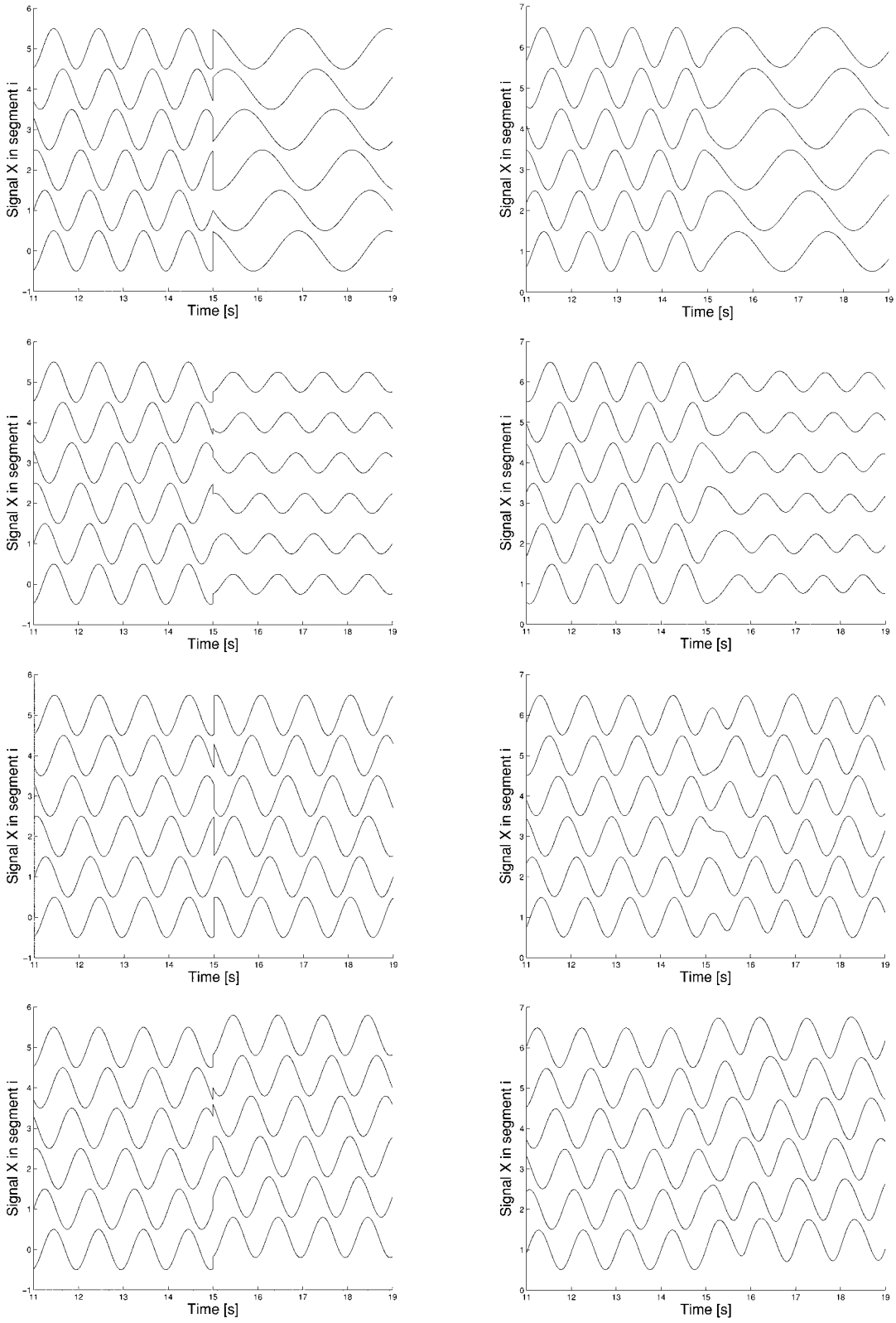

Fig. 14. Comparison between the sine-based controller (left) and the CPG-based controller (right). Top: Increase of period by a factor 2.0. Second from top: Decrease of amplitude by a factor 0.5. Third from top: Change of sign of the phase lag. Bottom: Modification of the offset x_0 by 0.3. All changes are made at t = 15 s.

but one should realize they only provide a first approximation. Some interaction forces such as contact forces, friction forces, and hydrodynamic forces are extremely difficult to simulate correctly, especially for articulated bodies that move and change shape. Using a robot means that the physical laws do not need to be simulated, and reduces the risk of numerical artifacts. In our case, the amphibious snake robot is a key tool for testing swimming gaits and for validating the simulation results. The same holds for perception: the use of real sensors (e.g., cameras) in a real environment eliminates the need to simulate the richness (in terms of noise, variations, and energy spectrum) of sensory inputs due to the real world.

Another interesting aspect of using robots is that they allow one to evaluate a computational model by comparing its results with biological data at multiple levels: from neuronal activity, to EMG recordings, to kinematics studies, and up to behavioral studies.

Finally, using robots forces one to aim at a comprehensive understanding of the functioning of a system. Failure is very visible with a robot (e.g., it will fall over or get stuck) and all the components of the control system have to be in place for the robot to work properly. For example, in the case of locomotion this requires correctly solving the problems of rhythm generation, co-ordination between degrees of freedom, control of balance, and modulation of speed and direction. This requirement to be comprehensive reduces the risks of wrongly assuming that some key computation is performed by another component than the one under study.

In our particular case, the main contribution of the lamprey and salamander robots to neurobiology is to test whether the signals produced by the CPG models can actually generate effective gaits in water and on ground, and to compare the resulting gaits with kinematics data from the real animals. For this the robots are a key complement to the dynamic simulation in order to quantitatively and reliably assess the realism of our models. Particularly interesting is the possibility to explore the relations between the types of undulations used by the animals and the speed and mechanical energy consumption of their locomotion. This will provide indications on what criteria are optimized when an animal chooses a particular gait.

One should however not underestimate the difficulties in using robots for computational neuroscience. First of all, it is very difficult to correctly replicate the biomechanical properties of animal bodies, in particular their number of degrees of freedom, their mass distribution, and their visco-elastic properties. The benefits of not needing to simulate the physics are therefore counterbalanced by the fact that the robot might present an intrinsic dynamics, which is significantly different from the modeled animal. In our case, for instance, the high gear reduction factor currently used in our snake robot means that it is much more rigid that the bodies of a lamprey or a salamander (the next prototype will have more powerful motors and lower gear reduction). Similarly, whereas some sensor modalities can correctly approximate biological ones, like vision and sound processing, others, like touch and proprioception, are yet far from being correctly replicated by current sensor technologies. Compared with simulations, robots present several additional constraints including: (1) being less adjustable, (2) requiring a large overhead for construction and maintenance, and (3) being less amenable to extensive experiments.

In conclusion, the pros and cons of using robots for computational neuroscience have to be carefully weighted. In our case, the robotic implementations and the simulations are complementary. One of the main interests of having the robot is to validate the physics-based simulation, to identify how a specific gait affects the speed and energy consumption of

locomotion and to further test the models in a complete sensing-to-acting loop. Additionally, the robot provides a good demonstration of how principles from neurobiology can contribute to robotics. The concept of CPGs constitutes an efficient and elegant way of dealing with several problems linked to locomotion control, namely, the online generation of coordinated joint angle trajectories for multiple degrees of freedom, the inclusion of sensory feedback, and the possibility to smoothly adjust the speed and direction of locomotion.

Acknowledgments

We would like to acknowledge support from the French "Ministère de la Recherche et de la Technologie" (program "ACI Neurosciences Intégratives et Computationnelles") and from a Swiss National Science Foundation Young Professorship grant to Auke Ijspeert. We are grateful to André Guignard and André Badertscher for their help in the design and construction of the robot.

References

Ashley-Ross, M. (1994a) Hindlimb kinematics during terrestrial locomotion in a salamander (dicampton tenebrosus). J. Exp. Biol. 193, 255–283.

Ashley-Ross, M. (1994b) Metamorphic and speed effects on hindlimb kinematics during terrestrial locomotion in the salamander (dicampton tenebrosus). J. Exp. Biol. 193, 285–305.

Ashley-Ross, M. and Bechtel, B. (2004) Kinematics of the transition between aquatic and terrestrial locomotion in the newt *Taricha torosa*. J. Exp. Biol. 207, 461–474.

Ashley-Ross, M. and Lauder, G. (1997) Motor patterns and kinematics during backward walking in the pacific giant salamander: evidence for novel motor output. J. Neurophys. 78, 3047–3060.

Ayers, J. and Crisman, J. (1993) The lobster as a model for an omnidirectional robotic ambulation control architecture. In: Biological Neural Networks in Invertebrate Neuroethology and Robotics. Beer, R., Ritzmann, R., and McKenna, T. (eds.) Academic Press, New York, pp. 287–316.

Bem, T., Cabelguen, J.-M., Ekeberg, O., and Grillner, S. (2003) From swimming to walking: a single basic network for two different behaviors. Biol. Cybern. 88, 79–90.

Bowtell, G. and Williams, T. (1991) Anguiliform body dynamics: modelling the interaction between muscle activation and body curvature. Phil. Trans. R. Soc. Lond. B. 334, 385–390.

Breithaupt, R., Dahnke, J., Zahedi, K., Hertzberg, J., and Pasemann, F. (2002) Robo-salamander—an approach for the benefit of both robotics and biology. In: Clawar (2002).

Buchanan, J. (1992) Neural network simulations of coupled locomotor oscillators in the lamprey spinal cord. Biol. Cybern. 66, 367–374.

Buchanan, J. and Grillner, S. (1987) Newly identified 'glutamate interneurons' and their role in locomotion in the lamprey spinal cord. Science 236, 312–314.

Cabelguen, J. M., Bourcier-Lucas, C., and Dubuc, R. (2003) Bimodal locomotion elicited by electrical stimulation of the midbrain in the salamander notophthalmus viridesecens. J. Neurosci. 23(6), 2434–2439.

Carling, J., Williams, T., and Bowtell, G. (1998) Self-propelled anguiliform swimming: simultaneous solution of the two dimensional Navier-Stokes equations and Newton's laws of motion. J. Exp. Biol. 201, 3143–3166.

Carrier, D. (1993) Action of the hypaxial muscles during walking and swimming in the salamander dicamptodon ensatus. J. Exp. Biol. 180, 75–63.

Cheng, J., Stein, R., Jovanovic, K., Yoshida, K., Bennett, D., and Han, Y. (1998) Identification, localization, and modulation of neural networks for walking in the mudpuppy (necturus maculatus) spinal cord. J. Neurosci. 18(11), 4295–4304.

Cohen, A. (1988) Evolution of the vertebrate central pattern generator for locomotion. In Neural Control of Rhythmic Movements in Vertebrates. Cohen, A. H., Rossignol, S., and Grillner, S. (eds.) John Wiley & Sons, New York.

Cohen, A. and Wallen, P. (1980) The neural correlate of locomotion in fish. "fictive swimming" induced in an in vitro preparation of the lamprey spinal cord. Exp. Brain Res. 41, 11–18.

Collins, J. and Richmond. (1994) Hard-wired central pattern generators for quadrupedal locomotion. Biol. Cybern. 71, 375–385.

Crespi, A., Badertscher, A., Guignard, A., and Ijspeert, A. (2005a) Swimming and crawling with an amphibious snake robot. In: IEEE International

Conference on Robotics and Automation (ICRA2005) 50(4), 3035–3039.
Crespi, A., Badertscher, A., Guignard, A., and Ijspeert, A. (2005b) AmphiBot I: an amphibious snake-like robot. Robot. Auton. Syst. (In press)
Deliagina, T., Zelenin, P., Fagerstedt, P., Grillner, S., and Orlovsky, G. (2000) Activity of the reticulospinal neurons during locomotion in freely behaving lamprey. J. Neurophys. 83, 853–863.
Delvolvé, I., Bem, T., and Cabelguen, J.-M. (1997) Epaxial and limb muscle activity during swimming and terrestrial stepping in the adult newt, *Pleurodeles Waltl*. J. Neurophys. 78, 638–650.
Delvolvé, I., Branchereau, P., Dubuc, R., and Cabelguen, J.-M. (1999) Fictive rhythmic motor patterns induced by NMDA in an in vitro brain stem-spinal cord preparation from an adult urodele. J. Neurophys. 82, 1074–1077.
Edwards, J. (1976) The evolution of terrestrial locomotion. In: Major Patterns in Vertebrate Evolution. Hecht, M. K, Goody, P. C, and Hecht, B. M. (eds.) Plenum Press, New York, pp. 553–577.
Ekeberg, O. (1993) A combined neuronal and mechanical model of fish swimming. Biol. Cybern. 69, 363–374.
Ekeberg, O., Wallén, P., Lansner, A., Traven, H., Brodin, L., and Grillner, S. (1991) A computer-based model for realistic simulations of neural networks I: The single neuron and synaptic interaction. Biol. Cybern. 65, 81–90.
Ermentrout, B. and Kopell, N. (1994) Inhibition-produced patterning in chains of coupled nonlinear oscillators. SIAM J. Appl. Math. 54(2), 478–507.
Frolich, L. and Biewener, A. (1992) Kinematic and electromyographic analysis of the functional role of the body axis during terrestrial and aquatic locomotion in the salamander *Ambystoma tigrinum*. J. Exp. Biol. 62, 107–130.
Fukuoka, Y., Kimura, H., and Cohen, A. (2003) Adaptive dynamic walking of a quadruped robot on irregular terrain based on biological concepts. Int. J. Robot. Res. 3–4, 187–202.
Gao, K. -Q. and Shubin, N. (2001) Late jurassic salamanders from northern china. Nature 410, 574–577.
Gillis, G. (1997) Anguiliform locomotion in an elongate salamander (siren intermedia): effects of speed on axial undulatory movements. J. Exp. Biol. 200, 767–784.
Grillner, S. (1985) Neural control of vertebrate locomotion-central mechanisms and reflex interaction with special reference to the cat. In: Feedback and Motor Control in Invertebrates and Vertebrates. Barnes, W. and Gladden. M. H. (eds.) Croom Helm, London, pp. 35–56.
Grillner, S., Buchanan, J., Wallén, P., and Brodin, L. (1988) Neural control of locomotion in lower vertebrates. In: Neural Control of Rhythmic Movements in Vertebrates. Cohen, A. H., Rossignol, S., and Grillner, S. (eds.) John Wiley & Sons, New York, pp. 1–40.
Grillner, S., Degliana, T., Ekeberg, O., et al. (1995) Neural networks that co-ordinate locomotion and body orientation in lamprey. Trends Neurosci. 18(6), 270–279.
Grillner, S., Wallén, P., and Brodin, L. (1991) Neuronal network generating locomotor behavior in lamprey: Circuitry, transmitters, membrane properties, and simulation. Annu. Rev. Neurosci. 14, 169–199.
Guan, L., Kiemel, T., and Cohen, A. (2001) Impact of movement and movement-related feedback on the lamprey central pattern generator for locomotion. J. Exp. Biol. 204, 2361–2370.
Hiraoka, A. and Kimura, H. (2002) A development of a salamander robot-design of a coupled neuromusculoskeletal system. In: Proceedings of the Annual Conference of the Robotics Society of Japan, Osaka.
Hirose, S. and Fukushima, E. (2002) Snakes and strings: New robotic components for rescue operations. In: Experimental Robotics VIII: Proceedings of the eight International Symposium ISER02. Siciliano, B. and Paolo, D. (eds.) Springer-Verlag, Berlin, pp. 48–63.
Ijspeert, A. (2001) A connectionist central pattern generator for the aquatic and terrestrial gaits of a simulated salamander. Biol. Cybern. 84(5), 331–348.
Ijspeert, A., Nakanishi, J., and Schaal, S. (2002) Movement imitation with nonlinear dynamical systems in humanoid robots. In: IEEE International Conference on Robotics and Automation (ICRA2002) pp. 1398–1403.
Ijspeert, A. J., Nakanishi, J., and Schaal, S. (2003) Learning control policies for movement imitation and movement recognition. In: Neural Information Processing System 15. Becker, S. T. S. and Obermayer, K. (eds.) pp. 1547–1554.
Kiemel, T., Gormley, K., Guan, L., Williams, T., and Cohen, A. (2003) Estimating the strength and direction of functional coupling in the lamprey spinal cord. J. Comput. Neurosci. 15, 233–245.

Kopell, N. (1995) Chains of coupled oscillators. In: The handbook of brain theory and neural networks. Arbib, M. (ed.) MIT Press, Cambridge, MA. pp. 178–183.

Lewis, M. (1996) Self-organization of locomotory controllers in robots and animals. Doctoral dissertation, Faculty of the Graduate School, University of Southern California. (unpublished).

McClellan, A. and Sigvardt, K. (1988) Features of entrainment of spinal pattern generators for locomotor activity in the lamprey spinal cord. J. Neurosci. 8, 133–145.

McIsaac, K. and Ostrowski, J. (1999) A geometric approach to anguilliform locomotion: Simulation and experiments with an underwater eel-robot. In: Icra 1999: Proceedings of 1999 IEEE International Conference on Robotics and Automation. pp. 2843–2848.

Ottoson, D. (1976) Morphology and physiology of muscle spindles. In: Frog neurobiology, a Handbook (Llinas, R. and Precht, W., eds.) Springer-Verlag, Berlin. pp. 643–675.

Pratt, J., Chew, C., Torres, A., Dilworth, P., and Pratt, G. (2001) Virtual model control: An intuitive approach for bipedal locomotion. Int. J. Robot. Res. 20(2), 129–143.

Roth, G., Nishikawa, K., Naujoks-Manteuffel, C., Schmidt, A., and Wake, D. (1993) Paedomorphosis and simplification in the nervous system of salamanders. Brain Behav. Evol. 42, 137–170.

Roth, G., Nishikawa, K., and Wake, D. (1997) Genome size, secondary simplification, and the evolution of the brain in salamanders. Brain Behav. Evol. 50, 50–59.

Saranli, U., Buehler, M., and Koditschek, D. (2001) RHex—a simple and highly mobile hexapod robot. Int. J. Robot. Res. 20(7), 616–631.

Schroeder, D. and Egar, M. (1990) Marginal neurons in the urodele spinal cord and the associated denticulate ligaments. J. Comp. Neurol. 301, 93–103.

Székely, G. and Czéh, G. (1976) Organization of locomotion. In: Frog Neurobiology, a Handbook. Springer-Verlag, Berlin, pp. 765–792.

Taga, G. (1998) A model of the neuro-musculo-skeletal system for anticipatory adjustment of human locomotion during obstacle avoidance. Biol. Cybern. 78(1), 9–17.

Taga, G., Yamaguchi, Y., and Shimizu, H. (1991) Self-organized control of bipedal locomotion by neural oscillators in unpredictable environment. Biol. Cybern. 65, 147–159.

Viana Di Prisco, G., Wallén, P., and Grillner, S. (1990) Synaptic effects of intraspinal stretch receptor neurons mediating movement-related feedback during locomotion. Brain Res. 530, 161–166.

Vukobratovic, M. and Borovac, B. (2004) Zero-moment point–thirty five years of life. Int. J. Hum. Robot. 1(1), 157–173.

Wallén, P., Ekeberg, O., Lansner, A., Brodin, L., Traven, H., and Grillner, S. (1992). A computer-based model for realistic simulations of neural networks II: The segmental network generating locomotor rhythmicity in the lamprey. J. Neurophys. 68, 1939–1950.

Webb, B. (2001) Can robots make good models of biological behaviour? Behav. Brain Sci. 24(6), 1033–1050.

Webb, B. (2002) Robots in invertebrate neuroscience. Nature 417, 359–363.

Wheatley, M., Edamura, M., and Stein, R. (1992) A comparison of intact and in-vitro locomotion in an adult amphibian. Exp. Brain Res. 88, 609–614.

Wilbur, C., Vorus, W., Cao, Y., and Currie, S. (2002) Neurotechnology for biomimetic robots. In: (chap. A Lamprey-Based Undulatory Vehicle). Ayers, J. Davis, J. and Rudolph, A. (eds.) Bradford/MIT Press, Cambridge, London.

Williams, T. (1992) Phase coupling by synaptic spread in chains of coupled neuronal oscillators. Science 258, 662–665.

Williams, T. and Sigvardt, K. (1995) Spinal cord of lamprey: generation of locomotor patterns. In: The Handbook of Brain Theory and Neural Networks. Arbib, M. (ed.) MIT Press, Cambridge, London, pp. 918–921.

Williams, T., Sigvardt, K., Kopell, N., Ermentrout, G., and Rempler, M. (1990) Forcing of coupled nonlinear oscillators: studies of intersegmental co-ordination in the lamprey locomotor central pattern generator. J. Neurophys. 64, 862–871.